Title
CHARACTERISTICS OF PIGMENTED LESIONS IN TYPE 2 IDIOPATHIC MACULAR TELANGIECTASIA

Journal
Retina, 38(&NA;)

ISSN
0275-004X

Authors
Leung, Irene
Sallo, Ferenc B
Bonelli, Roberto
et al.

Publication Date
2018

DOI
10.1097/iae.0000000000001842

Peer reviewed

HHS Public Access

Author manuscript

Retina. Author manuscript; available in PMC 2019 January 01.

Published in final edited form as:

Retina. 2018 January ; 38(Suppl 1): S43–S50. doi:10.1097/IAE.0000000000001842.

Characteristics of pigmented lesions in type 2 idiopathic macular telangiectasia

Irene Leung[1A,9], **Ferenc B Sallo**[1A,2,*], **Roberto Bonelli**[3,4], **Traci E Clemons**[5], **Daniel Pauleikhoff**[6], **Emily Y Chew**[7], **Alan C Bird**[1B], **Tunde Peto**[8,9], and **the MacTel Study group**

[1A]Department of Research and Development, Moorfields Eye Hospital, London, United Kingdom

[1B]Inherited Eye Disease, Moorfields Eye Hospital, London, United Kingdom

[2]UCL Institute of Ophthalmology, London, United Kingdom

[3]Population Health and Immunity, Walter and Eliza Hall Institute of Medical Research, Parkville, Victoria, Australia

[4]Department of Medical Biology, The University of Melbourne, Melbourne, Australia

[5]The EMMES Corporation, Rockville, Maryland, USA

[6]St. Franziskus Hospital, Münster, Germany

[7]National Eye Institute, National Institutes of Health, Bethesda, Maryland, USA

[8]Queen's University Belfast Faculty of Medicine Health and Life Sciences, Belfast, UK

[9]NIHR Biomedical Research Center for Ophthalmology, at Moorfields Eye Hospital NHS Foundation Trust and UCL Institute of Ophthalmology, London, UK

Abstract

Purpose—Pigment in the mid-retina is a characteristic sign in type 2 idiopathic macular telangiectasia (MacTel), and is considered to characterize late stage of the disease. Our aim was to investigate its incidence, and relationship with risk factors of MacTel, including outer retinal vascularization (ORV) and subretinal neovascular proliferation (SRNV).

Methods—Pigment extent was measured in fundus autofluorescence images of 150 eyes of 75 MacTel probands, using the Region Finder tool of Heidelberg Eye Explorer. A linear mixed model was used to analyze the dynamics of pigment and its associations with other features of the phenotype. The relative incidence of pigment and of outer retinal ORV and SRNV were analyzed within the full MacTel Study cohort (1244 probands).

Results—Mean pigment area at baseline was 0.157 mm^2 (range= 0 – 1.295 mm^2, SD=0.228 mm^2, n=101). Progression demonstrated a nonlinear pattern ($p<0.001$) at an overall rate of 0.0177 mm^2/year and was associated with the initial plaque size and with SRNV. There was a strong

*Correspondence should be directed to: Ferenc B Sallo, MD, PhD, The Reading Center, Department of Research and Development, Moorfields Eye Hospital NHS Foundation Trust, 162 City Road, London, EC1V 2PD, UK, phone: +44 207 566 2815, Fax: +44 207 608 6925, fbsallo@gmail.com.

Proprietary interest: I Leung: none, FB Sallo: none, R Bonelli: none, TE Clemons: none, D Pauleikhoff: none, EY Chew: none, AC Bird: none, T Peto: none.

correlation between fellow eyes (p≤0.0001). In approximately 25% of all SRNV cases SRNV may coincide with or precede pigment.

Conclusion—Our data may be useful for refining the current system for staging disease severity in MacTel.

Keywords

degeneration; imaging; MacTel; pigment; Müller cells; OCT; retina; telangiectasia

Background

Type 2 Idiopathic Macular Telangiectasia (MacTel) is a bilateral, potentially blinding retinal disease of unknown etiology and pathogenesis, with no proven treatment at present.[1-3] As the name suggests, MacTel was long considered a vascular disease, as most signs of the disease apparent on biomicroscopy, color fundus photography (CF) and fluorescein angiography (FFA) record vascular features, including telangiectatic capillaries, dilated venules, blunted and right-angle veins, associated with outer retinal vascularization (ORV, analogous to that demonstrated in animals with neuroglial disease,[4, 5]), early phase fluorescein leakage and late phase staining. Later-stage complications may include subretinal neovascular proliferation (SRNV) with subequent scarring and atrophy. More recent imaging modalities and histological evidence have revealed the neurodegenerative aspects of the disease and have led to a shift in the paradigm of the pathogenesis towards a primarily neurodegenerative disease[3], with prominent involvement of retinal Müller cells.[6-8] Dual-wavelength autofluorescence (DWAF) showed a progressive loss/redistribution of luteal pigment.[9-12] Blue light reflectance imaging revealed higher reflectivity in a specific pattern within the parafovea, that closely matches that of luteal pigment loss.[13] Optical coherence tomography (OCT) demonstrated low-reflective spaces in the inner and the outer retina and progressive atrophy and restructuring of the outer retina, characterized by a discontinuity (‘break’) in the line attributed to the photoreceptor inner segment ellipsoids (ellipsoid zone, EZ)[14] and an apparent ‘collapse’ of the disorganized inner retina through this ‘break’ towards the retinal pigment epithelium.[15-17]

One clinical sign that was described early is the accumulation of pigment within the retina.[1] This pigment appears in CF images as brown, grey or black, typically presents temporal to the foveal center, and is always adjacent to abnormal blood vessels. In later disease it grows into ‘plaques’ located in the mid-retina.[18]

According to the current concept of the natural history of the disease, pigment is considered an obligatory sign of the disease, indeed stage 4 in the system devised (in 1993) by Gass and Blodi for staging disease severity in MacTel is defined by the presence of pigment alone.[2]

Pigment is detectable using multiple imaging modalities. In CF images it can be distinguished from scar tissue or retinal blood based on its color. In FFA images it blocks autofluorescence and appears dark. It is highly reflective in OCT scans, blocking the path of light and thus casting ‘shadows’ on tissues distal to its location. Its proximal edge is however indicative of its location within the retinal layers.

The full lateral extent of pigment plaques is very well demonstrated by fundus autofluorescence (FAF) imaging. Fundus autofluorescence emanates from components of lipofuscin within the retinal pigment epithelium (RPE).[19, 20] Pigment deposits within the retinal layers internal to the RPE block autofluorescent light and appear as localized areas of decreased FAF, usually surrounded by an area of increased FAF (an 'atrophic halo').[21]

Heidelberg Engineering incorporated in the native software of the Spectralis series of SLO(+OCT) machines (Heidelberg Eye Explorer, Heyex) a software tool for measuring the area of decreased autofluorescence in FAF images (Region Finder). This tool has been validated for measuring the area of geographic atrophy in age-related macular degeneration.[22, 23] However, Region Finder can also be used for measuring the size of any low-intensity lesion with a reasonably sharp gradient/boundary, including intraretinal pigment in MacTel.

Our aim was to investigate the presence and progression characteristics of abnormal pigmentation in the natural history of MacTel.

Participants and Methods

Study Participants

Patients with a confirmed diagnosis of MacTel were selected from the cohort of an international multicenter prospective natural history observational study of MacTel.[24] For an analysis of the involvement of pigment in the natural history of the disease, the grading database of the full MacTel cohort was analyzed. Out of 1244 right and an equal number of left eyes 488 and 447 eyes (39.2% and 35.9%) respectively demonstrated pigment at least at one point in time during follow-up. For a detailed analysis of pigment extent, patients were selected based on the presence of pigment and the availability of good quality CF, FA, AF and OCT imaging and at least one year of follow-up. The study protocol adhered to the tenets of the Declaration of Helsinki and was approved by respective local institutional ethics committee at each participating center. Written, informed consent was obtained from each participant after explanation of the nature of the study.

Imaging

Standard 30° stereoscopic field 2 (centered on the fovea) color, red-free (RF) and fluorescein angiographic images of the fundus were recorded digitally using fundus cameras. Fundus autofluorescence was recorded using Heidelberg Retina Angiograph II or Heidelberg Spectralis SLO(+OCT) scanning laser ophthalmoscope systems (Heidelberg Engineering GmbH, Heidelberg, Germany). Spectral domain OCT scans analyzed for the presence of an EZ break were either crosshair scans of the retina through the foveal center acquired using Heidelberg Spectralis OCT systems (Heidelberg Engineering, Heidelberg, Germany), or 5-line raster scans centered on the fovea, recorded using Carl Zeiss Meditec Cirrus SD-OCT4000 systems (Carl Zeiss Meditec, Dublin, CA, USA).

Phenotyping

Characteristics of the phenotype were analyzed using overlay grids according to the International Classification for ARM and AMD,[25] counting the number of subfields affected by each sign. Early-phase FFA images were graded for lateral extent of vascular abnormalities characteristic of type 2 MacTel including dilated retinal capillaries, telangiectatic vessels, dilated, blunted and right angle veins and fluorescein leakage. Late-phase FFA images were graded for extent of hyperfluorescence according to the same pattern as early FFA changes.[24]

The presence and position relative to the foveal center (on/off) of a break in the EZ (IS/OS line) was graded in horizontal SD-OCT B-scans traversing the fovea. The extent of intraretinal pigment was measured using the Region Finder tool of Heidelberg Eye Explorer (see Figure 3). Repeatability data for the use of Region Finder (in geographic atrophy and Stargardt disease) have been published previously.[23, 26] Hypo-autofluorescence due blockage by brown pigment or blood was intensely dark and well defined when compared with hypo-autofluorescence due to loss of pigment epithelium (due to background choroidal autofluorescence). CF/RF images were also used as adjuncts to differentiate lesions, the distinction between melanin and blood was made on the basis of color photographs.

Participants also had a comprehensive dilated ophthalmologic examination during which monocular visual acuity was measured after refraction was performed under a standardized protocol, using the Early Treatment Diabetic Retinopathy Study (ETDRS) LogMAR visual acuity charts at a distance of 4 meters.[24, 27, 28]

Statistical Methods

Grading data variables for fluorescein leakage on the level of the outer capillary meshwork or the RPE, loss of retinal transparency, presence of visible telangiectatic vessels, of blunted retinal veins, of dilated retinal vessels (arteries/capillaries/venules) and for the presence of a break in the Ellipsoid Zone on OCT were aggregated for the 9 subfields of the grading grid into one variable per respective characteristic.

A linear mixed effects model was used with two random intercepts, one for each participant and one for each eye of each participant. A random slope was used for each of the random intercepts. Diagnostic residuals plots were created to test the assumptions of the model. Given the hypothesis generation goal of this investigation, p-value of < 0.05 was accepted as statistically significant. Analyses were conducted using R v3.3.2 available under a GNU GPL v2 license (R Development Core Team, www.r-project.org).

Results

Pigment area measurements were performed (anonymized and masked from clinical data) in 150 eyes of 75 probands, over time, a total of 754 measurements (eyes × visits) were available for analysis. Fifty-four measurements were excluded due to the lack of matching epidemiological (clinical) information. A further 122 observations from unilateral pigment cases were excluded and 5 observations were excluded due to the lack of phenotypical

information (i.e. no gradeable imaging), resulting in a sample of 573 observations of 73 probands.

The mean age of participants at baseline was 61.38 years (SD= 8.73), 30 males (41%) and 43 females (59%). Mean visual acuity at baseline was 61.56 letters (SD=18.19), Snellen visual acuity equivalent: 20/50. The follow-up period ranged from 1-8 years with a mean of 4.77 years (SD=2.10).

Mean pigment area at baseline was 0.157 mm^2 (median=0.0610, range= 0 – 1.295 mm^2, SD=0.228 mm^2, n=101). The distribution of pigment area measurements was unimodal and strongly skewed to the right. However, this did not affect the regression modeling. Change over time was in all cases positive (an increase in area).

Results from a linear mixed model revealed a dynamic progression of pigment area at an approximate rate of 0.0177 mm^2/year ($p<0.001$, see Table, Supplemental Digital Content 1, results of an analysis of pigment plaque area based on a linear mixed model). The growth rate of pigment area appeared to be associated with the initial area size of the pigment plaque. Specifically, we found the pigment area to increase by 0.0618 mm^2 ($p<0.001$) faster per year for each unit increment in the initial area size of pigment, indicating an overall non-linear progression rate. We observed no appreciable differences between right and left eyes (results not shown).

Area being a squared measure, we performed a further linear mixed model to test (assuming circular lesions) whether also the plaque *radius* progression is dependent on the initial value.[29] The association was not statistically significant (β=-0.0035, SE=0.0065, DF=104.6188, T-statistics=-0.5381, p=0.5917). Excluding initial radial lesion size in the next iteration, the increase in lesion *radius* appeared linear and on average 0.0194 mm annually.

In a second model we analyzed the relationship between pigment area size and other characteristics (see Table, Supplemental Digital Content 2, The effect of other clinical signs on pigment area using a linear mixed model). Loss of retinal transparency and neovascularization were associated with significantly higher pigment area growth rates (b=0.001, p-value<0.001) and (b=0.0156, p-value=0.036) respectively. Interestingly, vascular signs like right-angle veins or visible telangiectatic vessels were significantly associated with a *reduced* growth rate of pigment area (b= -0.0067, p-value < 0.001 and b= -0.001, p-value = 0.032, respectively). In this model, gender, age and ethnicity did not significantly affect pigment area or its growth (results not shown).

We also performed an analysis of symmetry of pigment area (presented in Table, Supplemental Digital Content 3). Pigment area size in one eye was strongly correlated with pigment area size in the fellow eye (right eyes p=0.0001 and left eyes p<0.001). We found pigment area to significantly and inversely affect BCVA (see Table, Supplemental Digital Content 4, The effect of pigment plaque area on visual acuity). A unit (mm^2) increment in pigment area decreased visual acuity by 16.1923 ETDRS letters (p=0.008).

Our study sample was too small for a reliable analysis of the time to transition of unilateral cases of pigment to bilateral, however, based on 15 initially unilateral cases we observed a mean time to bilaterality of 2.32 years (SD=1.71).

Based on color fundus and OCT images acquired over time, pigment appears adjacent to and propagates along abnormal blood vessels in the outer retina. Subsequently it forms a pigment plaque in the mid-retina that appears to be contiguous with the pigment accumulation in the outer retina (Figures 1-2).

To assess the sequence of occurrence of pigment relative to neovascularization, grading data of both eyes (based on color and FFA images) of 1244 probands enrolled in the MacTel Natural History Observation and Registry Studies were analyzed in descriptive terms for the presence of clinical signs indicating neovascularization in the present or the past (signs of active SRNV or retinal scar/fibrosis due to earlier SRNV).

Signs of SRNV were present in a total of 150 right eyes (12.1%); of these in 114 (76%) already had SRNV at baseline, in 36 eyes (24%) SRNV developed during the follow up of the study. In 29 (81%) of the eyes developing SRNV during follow-up, pigment was observed prior to the appearance of SRNV, in 7 eyes (19%) it was not. In left eyes, SRNV was present in a total of 118 eyes (9.5%); of these in 86 (73%) had SRNV at baseline. In 32 left eyes (27%) SRNV developed during follow-up and in 22 (69%) of these with pigment already present. In 10 left eyes (31%) SRNV developed without preceding pigment. A detailed review and analysis of the phenotype in all available images of all modalities confirmed the findings of the grading in 6 right eyes (17%) and 7 left eyes (22%), in two of these left eyes SRNV and pigment were first observed at the same visit. In one eye the typical MacTel pigment developed in a non-adjacent retinal area after SRNV appeared.

Discussion

One characteristic neurodegenerative sign in type 2 Idiopathic Macular Telangiectasia is the presence of dark brown pigment plaques enveloping blood vessels, typically appearing located to the mid-retina, temporal to the foveal center,[1, 30] as has been well demonstrated in animal models in which Mueller cells are involved in the disease process.[4,5] Prior to the availability of OCT, the diagnosis of type 2 MacTel often used to be based on their presence. The perceived significance of pigment plaques is also reflected in the fact that its presence alone drives stage 4 in the disease severity staging system devised by Gass and Blodi in 1993.[2]

Meleth et al.[18] noted in a sample of 22 non-neovascular MacTel eyes followed for on average 42.5 months (range=12–79 months) a linear growth rate of $8.3\pm1.7\times10^3$ μm^2/month (mean±SEM) based on measurements in colour fundus photographs.

In our study we used Heidelberg Region Finder on greyscale autofluorescence images of a sample of overall 150 eyes imaged over a mean follow-up period of 7.8 years. Growth rate in pigment area showed a non-linear progression pattern at of 0.0177 mm^2/year but with a linear radial progression rate. Differences in methodology, sample size, follow-up period and analysis methods as well as the lack of a calibration of true retinal image size based on the

axial length and refractive power of each eye in either study may explain differences in growth estimates.

The presence of blunted and right-angle veins, i.e. blood vessels that traverse the retinal layers at an abnormally steep angle towards the outer retina is characteristic of the phenotype of MacTel type 2. An increasing number of experimental models suggest that a retinal Müller glial dysfunction or cell death may contribute to the formation of these vessels, possibly through dysregulated lipid and glucose photoreceptor energy metabolism.[4, 31-33] According to the current hypotheses of the pathogenesis of pigment plaques, when pigmented cells from the retinal pigment epithelium come into contact with these abnormal vessels, the RPE cells use these as a scaffolding and migrate along the vessels into the inner retina, where they start to proliferate and spread ("sideways" away from the vessels) along the retinal layers, approximately on the level of the outer plexiform/ inner nuclear layers. This may play a role in the nonlinearity of the growth pattern evident from our data, with a relatively lower growth rate in the phase of perivascular 'vertical' migration and an increase in growth rate once the pigment reaches the mid/inner retina and starts proliferating 'horizontally' - along the retinal layers away from the vessel walls (also see Figures 1-3).

A transmissive 'window defect' around the pigment plaques with a central vessel can often be seen (also see Figures 2-3) and may be interpreted as indicative of centripetal RPE cell migration towards the vessel at the plaque center, although the sheer mass of pigment plaques suggests cell proliferation as well. The propensity of RPE to ensheathe and migrate along blood vessels is well known and documented in other diseases including retinitis pigmentosa.[34, 35] This pigmentary 'sheath' may also provide support for the abnormal blood vessels, decreasing their permeability thus limiting the extent of hemorrhages, while increasing the propensity of the tissue in type 2 MacTel for fibrosis and tissue contraction.[17] It does not however appear to provide a protection from secondary subretinal neovascularization.

Consistent with the findings of Meleth et al.[18], our data indicate that in the majority (on average 75%) of cases pigment plaques precede subretinal neovascular proliferation. SRNV may however also appear simultaneously with pigment or with no MacTel-type pigment detectable prior to the incidence of SRNV. Furthermore, pigment clumps may also be associated with the secondary neovascularization itself and although pigment associated with SRNV has a somewhat different morphology (more convex/round lesions, smoother convex edges, not immediately adjacent to following the vessels), differentiating pigment secondary to MacTel from that secondary to SRNV can be challenging, and the two types of pigment may even coexist in the same eye. One limitation of our study is that we cannot exclude the possibility that some of the pigment area measured in eyes with neovascularization is in fact part of pigmentation secondary to the neovascular complex itself.

Based on the slow but consistent and linear area growth rate found in their data, Meleth et al. concluded that pigment clumping may be a useful indicator of disease severity and an outcome measure for longitudinal studies. Our data also indicate a consistent area growth,

but at a nonlinear rate, which demonstrates a strong correlation with initial pigment area. The radial increase in size however appears linear. The similarity of SRNV-related pigment to MacTel-type pigment confounds the picture. Neovascularization, driving stage 5 in the current Gass & Blodi staging system may occur simultaneously with or even precede pigment (which defines stage 4). All these factors need to be taken into account if pigment clumping is to be used as a measure of disease progression. We expect our data to contribute to refining the current system for staging disease severity.

Supplementary Material

Refer to Web version on PubMed Central for supplementary material.

Acknowledgments

Financial support: The authors wish to thank the Lowy Medical Research Institute (LMRI) for providing support for funding this study. The LMRI also participated in the approval of the manuscript. R.B. was supported by the Melbourne International Research Scholarship. This work was also supported by Victorian State Government Operational Infrastructure Support and Australian Government NHMRC IRIISS funding.

Appendix

Participating Principal Investigators and Centers in the MacTel Study

Jose-Alain Sahel, MD, PhD, Center Hopitalier National D'Optalmologie des Quinze-Vingts, Paris, France;

Robyn Guymer, MD, Center for Eye Research, East Melbourne, Australia;

Gisele Soubrane, MD, PhD, FEBO, Clinique Ophtalmolgie de Creteil, Creteil, France;

Alain Gaudric, MD, Hopital Lariboisiere, Paris, France;

Steven Schwartz, MD, Jules Stein Eye Institute, UCLA, Los Angeles, CA (USA);

Ian Constable, MD, Lions Eye Institute, Nedlands, Australia;

Michael Cooney, MD, MBA, Manhattan Eye, Ear, & Throat Hospital, New York, NY (USA);

Catherine Egan, MD, Moorfields Eye Hospital, London, England (UK);

Lawrence Singerman, MD, Retina Associates of Cleveland, Cleveland, OH (USA);

Mark C Gillies, MD, PhD, Save Sight Institute, Sydney, Australia;

Martin Friedlander, MD, PhD, Scripps Research Institute, La Jolla, CA (USA);

Daniel Pauleikhoff, Prof. Dr., St. Franziskus Hospital, Muenster, Germany;

Joseph Moisseiev, MD, Goldschleger Eye Institute, Tel Hashomer, Israel;

Richard Rosen, MD, New York Eye and Ear Infirmary, New York, NY (USA);

Robert Murphy, MD, Retina Group of Washington, Fairfax, VA (USA);

Frank Holz, MD, University of Bonn, Bonn Germany;

Grant Comer, MD, University of Michigan, Kellogg Eye Center, Ann Arbor, MI (USA);

Barbara Blodi, MD, University of Wisconsin, Madison, WI (USA);

Diana Do, MD, Wilmer Eye Institute, Baltimore, MD (USA);

Alexander Brucker, MD, Scheie Eye Institute, Philadelphia, PA (USA);

Raja Narayanan, MD, LV Prasad Eye Institute, Hyderabad, India;

Sebastian Wolf, MD, PhD, University of Bern, Bern, Switzerland;

Philip Rosenfeld, MD, PhD, Bascom Palmer, Miami, FL (USA).

Paul S Bernstein, MD, PhD, Moran Eye Center, University of Utah, UT (USA)

Joan W Miller, MD, Massachusetts Eye and Ear Infirmary, Harvard Medical School, Boston, MA (USA)

References

1. Gass JD, Oyakawa RT. Idiopathic juxtafoveolar retinal telangiectasis. Arch Ophthalmol. 1982; 100:769–780. [PubMed: 7082207]
2. Gass JD, Blodi BA. Idiopathic juxtafoveolar retinal telangiectasis. Update of classification and follow-up study. Ophthalmology. 1993; 100:1536–1546. [PubMed: 8414413]
3. Charbel Issa P, Gillies MC, Chew EY, et al. Macular telangiectasia type 2. Prog Retin Eye Res. 2013; 34:49–77. [PubMed: 23219692]
4. Zhao M, Andrieu-Soler C, Kowalczuk L, et al. A new CRB1 rat mutation links Muller glial cells to retinal telangiectasia. J Neurosci. 2015; 35:6093–6106. [PubMed: 25878282]
5. Dorrell MI, Aguilar E, Jacobson R, et al. Antioxidant or neurotrophic factor treatment preserves function in a mouse model of neovascularization-associated oxidative stress. J Clin Invest. 2009; 119:611–623. [PubMed: 19188685]
6. Powner MB, Gillies MC, Tretiach M, et al. Perifoveal muller cell depletion in a case of macular telangiectasia type 2. Ophthalmology. 2010; 117:2407–2416. [PubMed: 20678804]
7. Powner MB, Gillies MC, Zhu M, Vevis K, Hunyor AP, Fruttiger M. Loss of Muller's cells and photoreceptors in macular telangiectasia type 2. Ophthalmology. 2013; 120:2344–2352. [PubMed: 23769334]
8. Reichenbach A, Bringmann A. New functions of Muller cells. Glia. 2013; 61:651–678. [PubMed: 23440929]
9. Zeimer MB, Spital G, Heimes B, Lommatzsch A, Pauleikhoff D. Macular telangiectasia--changes in macular pigment optical density during a 5-year follow-up. Retina. 2014; 34:920–928. [PubMed: 24150241]
10. Helb HM, Charbel Issa P, VDV RL, Berendschot TT, Scholl HP, Holz FG. Abnormal macular pigment distribution in type 2 idiopathic macular telangiectasia. Retina. 2008; 28:808–816. [PubMed: 18536596]

11. Esposti SD, Egan C, Bunce C, Moreland JD, Bird AC, Robson AG. Macular Pigment Parameters in Patients with Macular Telangiectasia (MacTel) and Normal Subjects: Implications of a Novel Analysis. Invest Ophthalmol Vis Sci. 2012; 53:6568–6575. [PubMed: 22899764]
12. Charbel Issa P, van der Veen RL, Stijfs A, Holz FG, Scholl HP, Berendschot TT. Quantification of reduced macular pigment optical density in the central retina in macular telangiectasia type 2. Exp Eye Res. 2009; 89:25–31. [PubMed: 19233170]
13. Charbel Issa P, Berendschot TT, Staurenghi G, Holz FG, Scholl HP. Confocal blue reflectance imaging in type 2 idiopathic macular telangiectasia. Invest Ophthalmol Vis Sci. 2008; 49:1172–1177. [PubMed: 18326746]
14. Spaide RF, Curcio CA. Anatomical correlates to the bands seen in the outer retina by optical coherence tomography: literature review and model. Retina. 2011; 31:1609–1619. [PubMed: 21844839]
15. Gaudric A, Ducos de Lahitte G, Cohen SY, Massin P, Haouchine B. Optical coherence tomography in group 2A idiopathic juxtafoveolar retinal telangiectasis. Arch Ophthalmol. 2006; 124:1410–1419. [PubMed: 17030708]
16. Albini TA, Benz MS, Coffee RE, et al. Optical coherence tomography of idiopathic juxtafoveolar telangiectasia. Ophthalmic Surg Lasers Imaging. 2006; 37:120–128. [PubMed: 16583633]
17. Sallo FB, Peto T, Egan C, et al. The IS/OS junction layer in the natural history of type 2 idiopathic macular telangiectasia. Invest Ophthalmol Vis Sci. 2012; 53:7889–7895. [PubMed: 23092925]
18. Meleth AD, Toy BC, Nigam D, et al. Prevalence and progression of pigment clumping associated with idiopathic macular telangiectasia type 2. Retina. 2013; 33:762–770. [PubMed: 23064429]
19. Delori FC, Dorey CK. In vivo technique for autofluorescent lipopigments. Methods Mol Biol. 1998; 108:229–243. [PubMed: 9921533]
20. Delori FC, Dorey CK, Staurenghi G, Arend O, Goger DG, Weiter JJ. In vivo fluorescence of the ocular fundus exhibits retinal pigment epithelium lipofuscin characteristics. Invest Ophthalmol Vis Sci. 1995; 36:718–729. [PubMed: 7890502]
21. Wong WT, Forooghian F, Majumdar Z, Bonner RF, Cunningham D, Chew EY. Fundus autofluorescence in type 2 idiopathic macular telangiectasia: correlation with optical coherence tomography and microperimetry. Am J Ophthalmol. 2009; 148:573–583. [PubMed: 19573860]
22. Schmitz-Valckenberg S, Brinkmann CK, Alten F, et al. Semiautomated image processing method for identification and quantification of geographic atrophy in age-related macular degeneration. Invest Ophthalmol Vis Sci. 2011; 52:7640–7646. [PubMed: 21873669]
23. Panthier C, Querques G, Puche N, et al. Evaluation of semiautomated measurement of geographic atrophy in age-related macular degeneration by fundus autofluorescence in clinical setting. Retina. 2014; 34:576–582. [PubMed: 24056526]
24. Clemons TE, Gillies MC, Chew EY, et al. Baseline characteristics of participants in the natural history study of macular telangiectasia (MacTel) MacTel Project Report No. 2. Ophthalmic Epidemiol. 17:66–73.
25. Bird AC, Bressler NM, Bressler SB, et al. An international classification and grading system for age-related maculopathy and age-related macular degeneration. The International ARM Epidemiological Study Group. Surv Ophthalmol. 1995; 39:367–374. [PubMed: 7604360]
26. Kuehlewein L, Hariri AH, Ho A, et al. Comparison of Manual and Semiautomated Fundus Autofluorescence Analysis of Macular Atrophy in Stargardt Disease Phenotype. Retina. 2016; 36:1216–1221. [PubMed: 26583307]
27. Ferris FL 3rd, Kassoff A, Bresnick GH, Bailey I. New visual acuity charts for clinical research. Am J Ophthalmol. 1982; 94:91–96. [PubMed: 7091289]
28. Early Treatment Diabetic Retinopathy Study design and baseline patient characteristics. ETDRS report number 7. Ophthalmology. 1991; 98:741–756. [PubMed: 2062510]
29. Feuer WJ, Yehoshua Z, Gregori G, et al. Square root transformation of geographic atrophy area measurements to eliminate dependence of growth rates on baseline lesion measurements: a reanalysis of age-related eye disease study report no. 26. JAMA ophthalmology. 2013; 131:110–111. [PubMed: 23307222]
30. Gass, JDM. Stereoscopic atlas of macular diseases : diagnosis and treatment. 2d ed.. Vol. xi. St. Louis: C. V. Mosby; 1977. p. 411

31. Chung SH, Shen W, Jayawardana K, et al. Differential gene expression profiling after conditional Muller-cell ablation in a novel transgenic model. Invest Ophthalmol Vis Sci. 2013; 54:2142–2152. [PubMed: 23449719]

32. Shen W, Fruttiger M, Zhu L, et al. Conditional Mullercell ablation causes independent neuronal and vascular pathologies in a novel transgenic model. J Neurosci. 2012; 32:15715–15727. [PubMed: 23136411]

33. Joyal JS, Sun Y, Gantner ML, et al. Retinal lipid and glucose metabolism dictates angiogenesis through the lipid sensor Ffar1. Nat Med. 2016; 22:439–445. [PubMed: 26974308]

34. Li ZY, Possin DE, Milam AH. Histopathology of bone spicule pigmentation in retinitis pigmentosa. Ophthalmology. 1995; 102:805–816. [PubMed: 7777280]

35. Milam AH, Li ZY, Fariss RN. Histopathology of the human retina in retinitis pigmentosa. Prog Retin Eye Res. 1998; 17:175–205. [PubMed: 9695792]

Summary Statement

Dark brown pigment plaques are a frequent sign during the evolution of MacTel and their origin is most likely the retinal pigment epithelial cells migrating along penetrating vessels into the mid-retinal layers. The pigment area can be measured in AF images using Heidelberg Region Finder, its progression follows a non-linear pattern. Outer retinal vascularization may be observed before pigmentation.

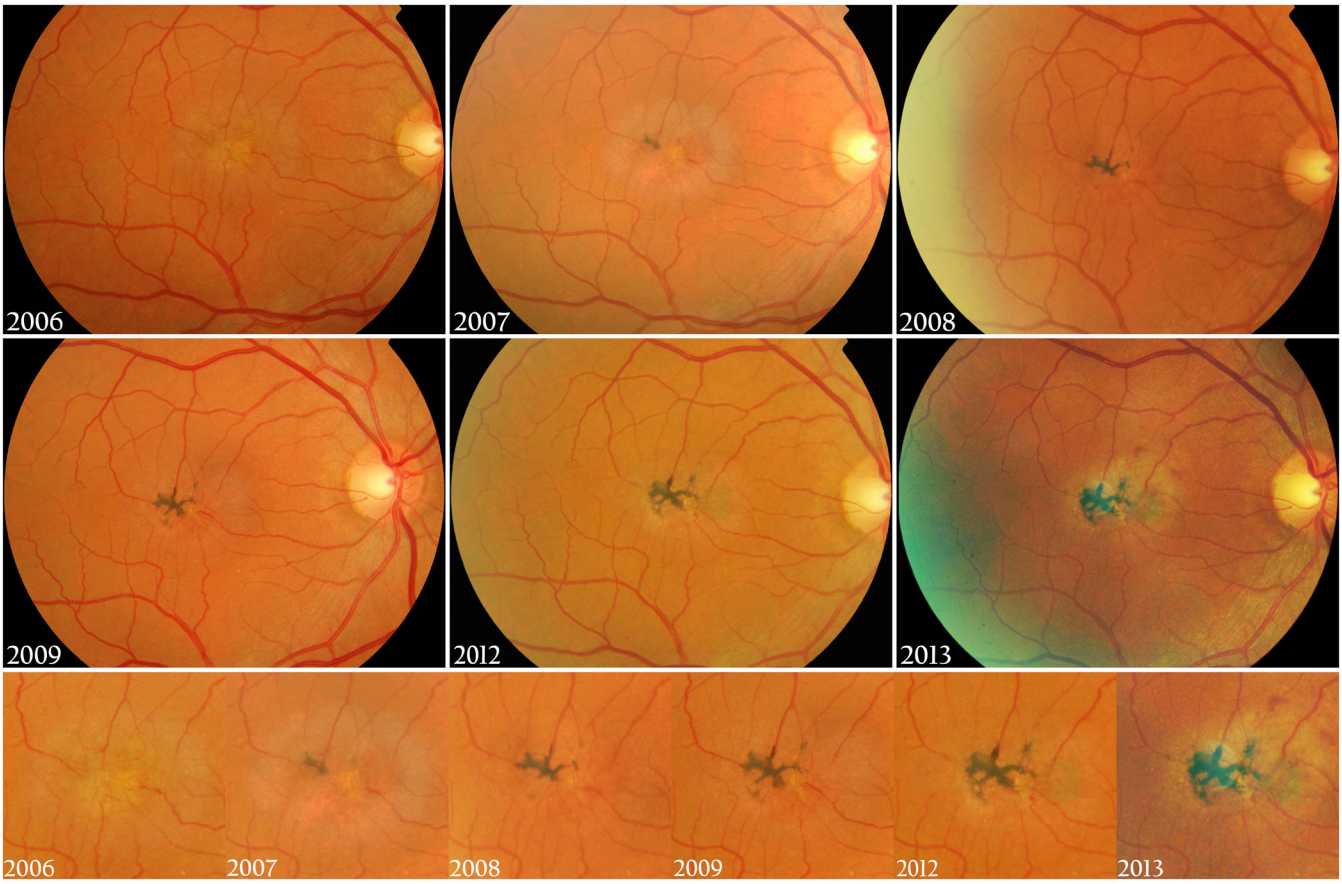

Figure 1. Progression of abnormal pigment in MacTel in color fundus images

Typically, brown (melanin-like) pigment first appears focally temporal of the foveal centre, involving abnormal outer retinal blood vessels. Over time it may extend to the foveal centre. Clearly visible pigment plaques are typically located to the mid-retina.

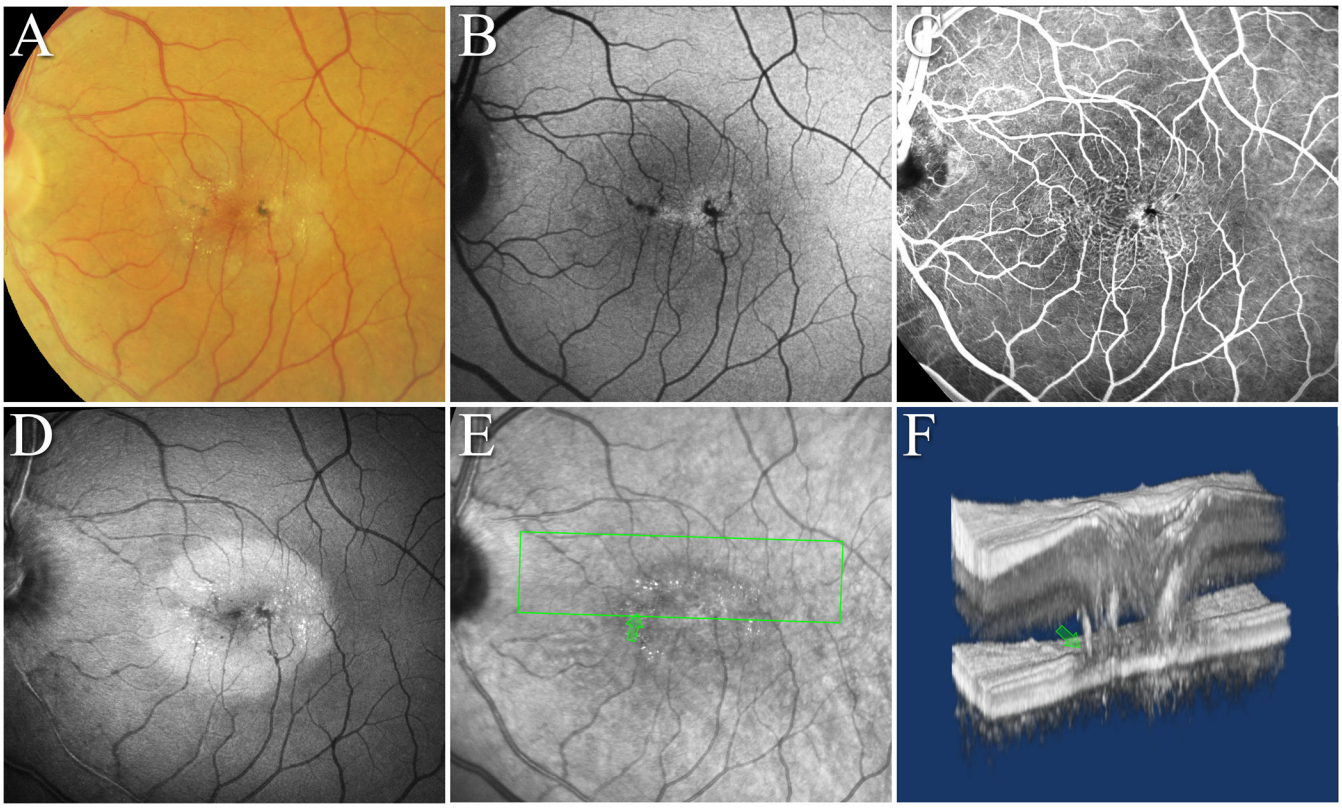

Figure 2. Typical MacTel pigment plaques in multiple imaging modalities

A. CF, **B.** autofluorescence, **C.** early FFA, **D.** blue light reflectance image, **E.** infrared and **F.**: 3D perspective view of OCT volume data. As the OCT perspective view illustrates, the intraretinal pigment is located surrounding abnormal blood vessels originating in the deep retinal plexus and traversing the retinal layers towards the RPE (matching green arrows). Most of the pigment in this eye is located external to the superficial and deep retinal meshworks, the apparent extent of the pigment is much smaller in the FFA image than in the FAF and CF images. The source of the pigment is hypothesized to be inside cells migrating from the RPE.

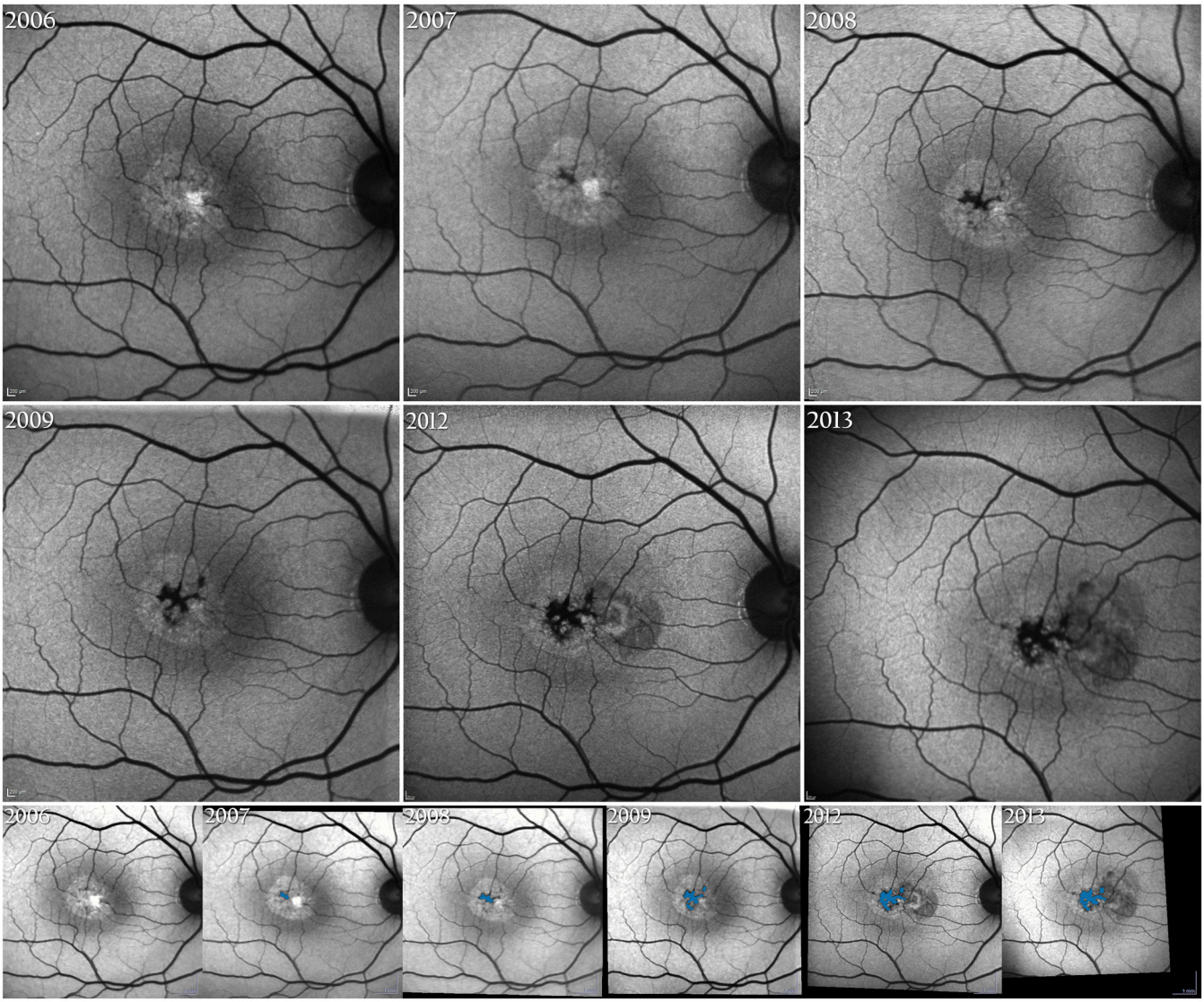

Figure 3. Top and Middle rows: Corresponding SLO AF images of the eye presented in Figure 1

Increased central AF due to loss of luteal pigment is apparent. Decreased AF (intense irregular dark areas) is caused by the masking effect of pigment in the mid-retina, involving abnormal blood vessels. This needs to be differentiated from dense scar tissue, blood or subretinal neovascular proliferation (2012-). Bottom row shows the pigment area progression captured by the Region Finder tool of Heidelberg Eye Explorer (blue area).